Heat and Mass Transfer
https://doi.org/10.1007/s00231-022-03210-5

ORIGINAL ARTICLE

Drying of *Spirulina* with a continuous infrared-assisted refractance window™ dryer equipped with a photovoltaic-thermal solar collector

Zeinab Rezvani[1] · Hamid Mortezapour[1] · Mehran Ameri[2] · Hamid-Reza Akhavan[3] · Selçuk Arslan[4]

Received: 4 July 2021 / Accepted: 30 March 2022
© The Author(s), under exclusive licence to Springer-Verlag GmbH Germany, part of Springer Nature 2022

Abstract

Drying is one of the effective techniques in increasing *Spirulina* shelf life. Performance of a continuous infrared-refractance window™ dryer coupled with a double-pass photovoltaic-thermal (PVT) solar collector was investigated at different drying air flow rates (0.036, 0.071, and 0.107 $m^3/s/m^2$ collector) and *Spirulina* feeding rates (1.2 L/h, 1.8 L/h, and 2.4 L/h). The maximum electrical and thermal efficiencies of the PVT collector, solar electricity fraction, and solar heat fraction were found to be 11.91%, 68.47%, 0.76, and 0.78, respectively. The average specific energy consumption values ranged between 1.21 and 2.437 kWh/kg. The yellowness index (b^*) of the dried products decreased by 63.67%, and the redness index (a^*) increased by 39.4% when the feeding rate was increased from 1.2 to 2.4 L/h. The highest phycocyanin content was approximately 11.4 g/100 g at the feeding rate of 2.4 L/h and the air flow rate of 0.107 $m^3/s/m^2$ collector.

Nomenclature

A	Area (m^2)
a*	Redness (dimensionless)
b	Width of PV panel (m)
b*	Yellowness (dimensionless)
C	Specific heat (J/kg K)
d	Depth of air channel (m)
D_h	Hydraulic diameter (m)
dt	Experiment time (s)
dx	Unit length (m)
E_{PV}	Electrical energy of the PV module during the tests (kJ)
E_{Sh}	Thermal energy produced in PVT collector (kJ)
E_T	Total energy consumption (kJ)
G	Solar irradiance (W/m^2)
H	Height of fin (m)
h	Heat transfer coefficient (W/m^2K)
k	Thermal conductivity (W/mk)
L	Length (m)
L*	Lightness (dimensionless)
l	Latent heat (kJ/kg)
m	Mass (kg)
$\dot{m}$	Mass flow rate (kg/s)
Nu	Nusselt number (dimensionless)
OD	Optical density
PF	Packing factor of PV panel (dimensionless)
P_{PV}	Electrical power generated by PVT collector (W)
$\dot{Q}$	Useful thermal power gain of PVT collector (W)
S	Radiative heat flux (W/m^2)
SEC	Specific energy consumption (kWh/kg)
SEF	Solar electricity fraction (decimal)
SHF	Solar heat fraction (decimal)

✉ Hamid Mortezapour
h.mortezapour@uk.ac.ir

Zeinab Rezvani
z.rezvani@agr.uk.ac.ir

Mehran Ameri
ameri_mm@uk.ac.ir

Hamid-Reza Akhavan
hr.akhavan@uk.ac.ir

Selçuk Arslan
sarslan@uludag.edu.tr

[1] Department of Biosystems Engineering, Faculty of Agriculture, Shahid Bahonar University of Kerman, Kerman, Iran

[2] Department of Mechanical Engineering, Faculty of Engineering, Shahid Bahonar University of Kerman, Kerman, Iran

[3] Department of Food Science and Technology, Faculty of Agriculture, Shahid Bahonar University of Kerman, Kerman, Iran

[4] Faculty of Agriculture, Department of Biosystems Engineering, Bursa Uludağ University, TR 16059 Bursa, Turkey

Published online: 08 April 2022

SMER	Specific moisture extraction rate (kg/kWh)
T	Temperature (K)
t	Thickness of fin (m)
U	Heat losses coefficient (w/m^{2}K)
UC	Uncertainty of instrument
V	Velocity of wind (m/s)
VVolume air fl	Ow rate (m^3/s/m^2 collector)
MF	Mass fraction (decimal)

Greek

α	Absorption coefficient (decimal)
δ	Width of Mylar (m)
ε	Emissivity (decimal)
ζ	Efficiency of PVT collector (decimal)
η_{fin}	Efficiency of fin (decimal)
σ	Stefan-Boltzmann constant (5.67×10^{-8} W/m^2 K^4)
τ	Transmission coefficient (decimal)
Φ	Effectiveness factor of fins (dimensionless)

Subscript

a	Drying air
amb	Ambient
au	Upper airstream
al	Lower airstream
bp	Back plate
c	Convective
el	Electrical
g	Glass
th	Thermal
i	Inlet air
IR	Infrared
o	Outlet air
p	Absorber plate
r	Radiative
s	Sky
SM	*Spirulina maxima*
sw	Side walls
v	Vaporization
w	Wind
wd	Evaporated water

1 Introduction

Spirulina is a green–blue alga of the cyanobacterial genus that is divided into two species, *Arthrospira maxima* and *Arthrospira plantensis*. Producing more than 30% of total production, *Spirulina* has the most extensive microalgae cultivation worldwide [1]. *Spirulina* is a good source of carotenoids, phycobiliprotein, and especially protein [2]. This microalga is known as a source of bacterial phycocyanin (C-PC) [3, 4]. *Spirulina* has been certified by the food and drug administration (FDA) of the USA as a safe food that can meet human nutritional need in the future [5]. Drying is one of the effective techniques in increasing *Spirulina* shelf life. There are several methods used to dry and dehydrate microalgae. The amount of phycocyanin may vary depending on the processing method.

The energy crisis and demand for high-quality products have increased the challenge among researchers to come up with new methods for food drying [6]. The main challenge of industrial dryers is their high energy consumption, which accounts for about 12 to 20% of energy needs in the industry [7]. On the other hand, the energy needed for dryers is usually supplied from fossil fuels. With rising environmental concerns due to fossil fuel consumption, alternative clean resources, especially solar energy, have received much attention. In this way, dryers equipped with solar collectors, especially photovoltaic- thermal (PVT) systems [8, 9], were designed and manufactured for various agricultural products. Photovoltaic (PV) cells, which are the most used among solar technologies, change a large part of the received solar beams into heat and a small part of it into electricity. As a result, productive power is declined. PVT technologies transfer the thermal energy of the PV panel surface in a fluid for low-temperature applications. Therefore, the panel is cooled and its efficiency is improved [8].

The water-bed dryer is a relatively new technology that uses thermal energy of hot water to dry heat-sensitive foods with low energy consumption, and very high quality. This type of dryer is known as refractance window (RW)™ dryer [7]. In the water-bed dryer, heat transfers to the product surface through conduction and radiation. Several researchers have compared the drying quality of RW™ dryers with other types of dryers. Goldenberry pulps were dried using RW, freeze, convection, and infrared (IR) drying methods to compare the final product quality. The product dried by the RW, despite its long duration, was very close to the freeze-dried product [10]. In the drying of apple, beef, and salmon using RW dryer, it was found that the mass transfer in beef and salmon by RW improved not as well as sliced apples [11].

The RW dryer has an intermediate transparent belt that works like a window. As the product's surface in contact with the belt goes dry, the belt acts like a closed window and limits the radiation heat transfer from the hot water to the product [12, 13]. Simultaneously, an air gap is created between the belt and the product surface that makes a significant thermal resistance and reduces the heat conduction to the product. Therefore, if the product is thick, in addition to increasing the drying time, a significant moisture difference happens between its upper and lower surfaces. To solve this problem, improve energy efficiency and decrease drying time, the use of IR radiation with the RW dryer was considered in the present study. Furthermore, a forced flow

of hot air supplied by a PVT collector was considered to dry the product uniformly and prevent surface burning. The PVT collector is supposed to produce some of the electrical energy required for the dryer while providing the heat needed for the passing air. RW dryers have gained a lot of attention in recent years. But there is no report in the literature regarding its combination with PVT systems and IR lamps. As a heat-sensitive product whose phycocyanin content is profoundly impressed by the drying method, *Spirulina* was used to investigate the proposed dryer performance experimentally. This study aims at investigating the electrical and thermal efficiencies of the PVT collector, solar electricity and heat fractions, specific energy consumption, specific moisture extraction rate, moisture content, color indices, and phycocyanin content of the *Spirulina* product.

2 Material and method

2.1 System description

The proposed dryer is divided into two main units; the PVT air collector, and the infrared-assisted refractance window™ (IRARW) dryer. The PVT collector has a double-pass configuration designed to provide thermal energy for the drying air, and a part of the electrical energy of the dryer. An exploded diagram of the designed collector is shown in Fig. 1. This unit includes a glass cover, PV module, two aluminum sheets, longitudinal fins, and horizontal blades. The fins are mounted longitudinally behind the PV module to work as the extended surfaces and enhance heat transfer rate. The horizontal fins, installed on the duct floor, are used to make a turbulent air flow. Fresh air is supplied to the PV collector through the top opening and moves down through the PV module. At the end of this path, the air returns through the longitudinal blades beneath the PV module. The collector was installed with a tilt angle of 30° due south.

The IRARW dryer includes a hot water bed, duct, belt conveyor, belt driver, hot water pump, blower, IR lamps, auxiliary tank, and water heater. A schematic of the IRARW dryer coupled with the PVT is shown in Fig. 2.

The belt was tightly wrapped on the top of the hot water bed in contact with the water. Along the drying path, the product loses its moisture and becomes dry under the influence of the bottom hot water bed, the above IR lamps, and the warmed air flow. Table 1 expresses the details of the dryer components.

The products are placed on the surface of the Mylar belt to move along the drying path, where they lose moisture and get dried under the influence of the bottom hot water bed, the above IR lamps, and the hot airflow. The heat transfers from the hot water to the product surface through conduction and radiation. The IR waves, emitted from the IR lamps, infiltrate into the product, resulting in a temperature difference

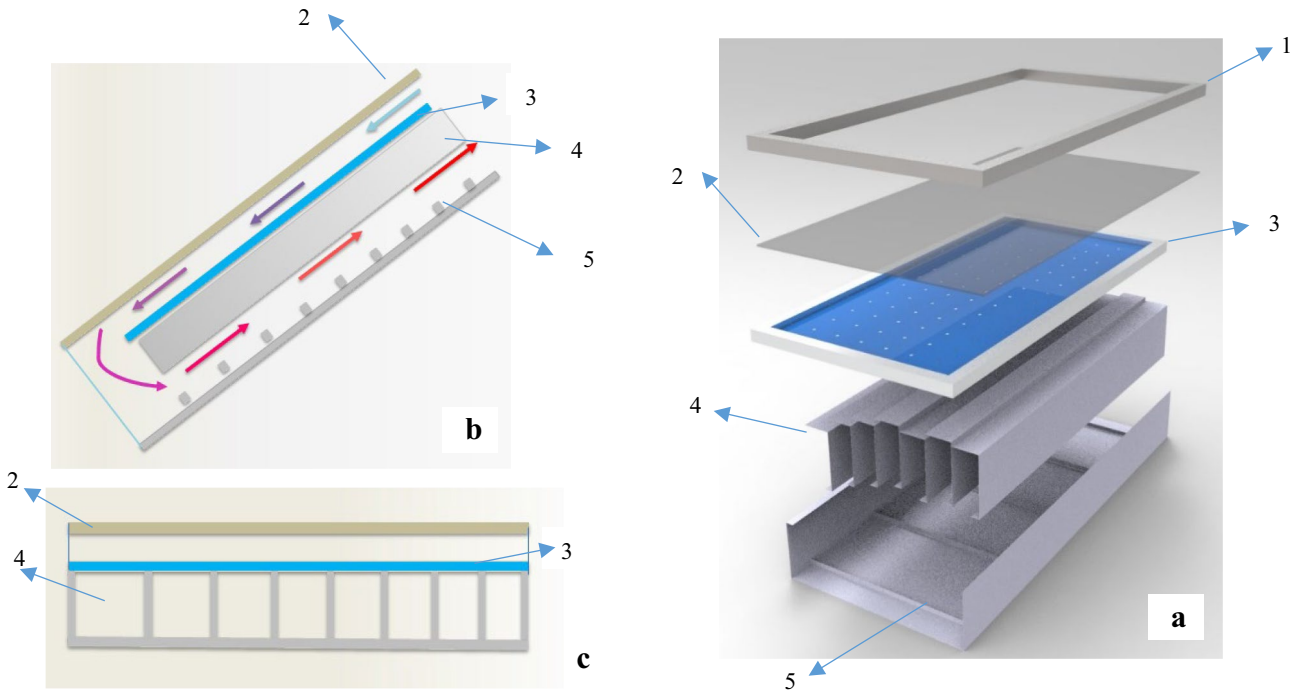


Fig. 1 Exploded view (**a**), longitudinal (**b**), and cross-sections of the double-pass PVT air collector (**c**): 1- Frame, 2- Glass cover, 3- PV panel, 4- Air channels, 5- Horizontal blades

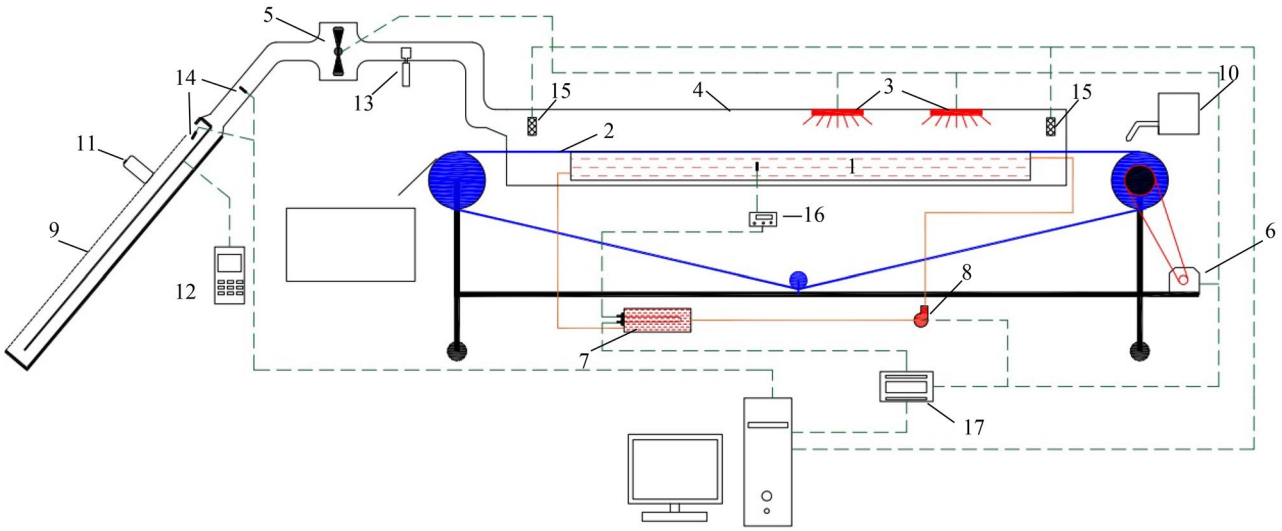


Fig. 2 A schematic of the continuous IRARW dryer: 1- Hot water bed, 2- Transparent polyester, 3- IR element, 4- Stainless steel duct, 5- Blower, 6- Electromotor (belt driver), 7- Water tank & water heater, 8- Hot water pump, 9- PVT collector, 10- *Spirulina* feeding system, 11- Pyranometer, 12- Solar power analyzer, 13- Anemometer, 14- Temperature sensor, 15- Relative humidity and temperature sensor, 16- Temperature controller, 17-Wattmeter transmitter

between the inside and the surface. This leads to an increase in the moisture flux and rapid saturation of the air surrounding the product surface. To provide a uniform light distribution on the belt, based on the method developed by Seyyed Abadi et al. [14], the lamps were installed on an adjustable frame that allowed changing the longitudinal distance between the lamps. The dryer is supported with an airflow to move out the saturated air surrounding the product.

2.2 Theoretical analysis

Mathematical formulation of the designed compound dryer has been conducted for the two main parts of the PVT solar collector and the IRARW dryer. For this purpose, energy balance equations of each component were developed, considering the following assumptions: a) the heat transfer is one dimensional, b) the components are in quasi-steady condition, c) there is no temperature difference between the PV panel and the absorber plate as well as between the Mylar and the product film, d) the air leakage through the collector duct is negligible, e) variation of the temperature of the collector component is only in the direction of the airflow, f) thermal capacity of the PV panel, absorber plate, back plate, glass, and Mylar is negligible, g) convective heat transfer coefficient of wind is constant around the collector, and h) the airflow in the system is steady, so its mass flow rate is constant throughout the flowing path. The energy balance equations of the different components are written as follows:

Table 1 Technical specifications of the dryer components

Apparatus	Specifications
Photovoltaic Panel	Polycrystalline, 180 W, $V_{max}=35.6$ V, $I_{max}=5.06$ A, 1.58 m×0.80 m×0.045 m
Charge controller	12–24 V, 30 A
Battery	2×12 V, 90 Ah
IR lamp	2×200 W, 220 V
Blower	40 W
Hot water bed	0.4 m×1.95 m×0.14 m
Transparent polyester	Mylar, 7 m×0.4 m×0.025 m
Stainless steel duct	0.52 m×0.7 m×3 m
Hot water pump	46 W, Flow rate: 0.5 L/min
Electromotor	14 W, 1 rpm
Water heater	Max 2000 W

a. **PV-T solar collector**

1. The glass cover [15–17]

$$\alpha_g G A_g + h_{c.au-g} A_g \left(T_{au} - T_g\right) + h_{r.p-g} A_g \left(T_P - T_g\right) = h_{r.g-s} A_g \left(T_g - T_s\right) + h_{c.w} A_g \left(T_g - T_w\right) \quad (1)$$

2. The upper airstream between the glass cover and the absorber plate [15, 16]

$$h_{c.p-au}\left(T_p - T_{au}\right)bdx + h_{c.g-al}\left(T_g - T_{al}\right)bdx = \dot{m}_a C_{au}\frac{dT_{au}}{dx}dx + U_{sw}(T_{au} - T_{amb})\,ddx \quad (2)$$

where U_{sw}, the overall heat loss coefficient from the side walls, can be written as following [18]:

$$U_{sw} = \frac{1}{\frac{1}{h_{c.au-sw}} + \frac{L_{sw}}{k_{sw}} + \frac{1}{h_w}} \tag{3}$$

3. The absorber plate and the PV panel [15]

$$\begin{aligned}&\tau_g^2\alpha_p G(1-PF)A_p + \tau_g^2\alpha_{cell}G(PF)(\zeta_{el}-1)A_p \\ &= h_{c.p-au}(T_p - T_{au})A_p + h_{r.p-g}A_p(T_p - T_g) \\ &\quad + h_{c.p-al}\varnothing A_P(T_P - T_{al}) + h_{r.p-bp}A_p(T_p - T_{bp})\end{aligned} \tag{4}$$

where electrical efficiency and packing factor of the PV panel are given by the following expressions [19].

$$\zeta_{el} = 0.125\left[1 - 0.004(T_p - 293)\right] \tag{5}$$

$$PF = \frac{A_{cell}}{A_p} \tag{6}$$

The effectiveness factor of fins (∅) can be calculated as follow [20, 21]:

$$\varnothing = 1 + \frac{A_{fin}}{A_P}\eta_{fin} \tag{7}$$

where $\eta_{fin} = \tanh\frac{\sqrt{\frac{2h_{c.al}H}{k_{fin}t}}}{\frac{2h_{c.al}H}{k_{fin}t}}$

4. The lower airstream between the fined absorber plate and the back plate [15]

$$\begin{aligned}h_{c.p-al}\varnothing(T_p - T_{al})bdx &= \dot{m}_{al}C_{al}\frac{dT_{al}}{dx}dx \\ &\quad + h_{c.al-bp}(T_{al} - T_{bp})bdx \\ &\quad + U_{sw}(T_{al} - T_{amb})\,ddx\end{aligned} \tag{8}$$

5. The back plate [15]

$$h_{c.bp-al}(T_{al} - T_{bp})A_p + h_{r.p-bp}(T_p - T_{bp})A_p = U_{bp}(T_{bp} - T_{amb})A_p \tag{9}$$

where the overall heat transfer coefficient from the back plate to ambient (U_{bp}) is [21]:

$$U_{bp} = \frac{1}{\frac{L_{bp}}{k_{bp}} + \frac{1}{h_w}} \tag{10}$$

The other parameters of the above expressions can be given as follows [15, 21]:

$$T_s = 0.0552T_{amb}^{1.5} \tag{11}$$

$$h_{c.w} = 5 \cdot 67 + 3 \cdot 8V \tag{12}$$

$$h_{r.g-s} = \varepsilon_g\sigma(T_g^2 + T_s^2)(T_g + T_s) \tag{13}$$

$$h_{r.p-g} = \frac{\sigma(T_p^2 + T_g^2)(T_p + T_g)}{\left(\frac{1}{\varepsilon_p}\right) + \left(\frac{1}{\varepsilon_g}\right)^{-1}} \tag{14}$$

$$h_c = \frac{Nu_a k_a}{D_h} \tag{15}$$

$$D_h = \frac{2bd}{b+d} \tag{16}$$

b. **IR- assisted refractance window™ dryer**

The energy balance equation for the product film on the Mylar can be written as the following expression [21].

$$\begin{aligned}l_v\frac{dm_{SM}}{dx}dx + \dot{m}_{SM}C_{SM}\frac{dT_{SM}}{dx}dx &= h_{c.SM-a}(T_a - T_{SM})\delta\,dx \\ &\quad + k_M\frac{T_{SM} - T_M}{l_M}\delta dx + h_{r.water-SM}(T_{water} - T_{SM})\delta\,dx \\ &\quad + \alpha_{SM}S_{IR}\delta\,dx\end{aligned} \tag{17}$$

where radiative heat transfer coefficient between hot water and the *Spirulina maxima*, and the specific heat of the *Spirulina maxima* are obtained as follows [21, 22]:

$$h_{r.SM-water} = \varepsilon\sigma(T_{water} + T_{SM})(T_{water}^2 + T_{SM}^2) \tag{18}$$

$$\begin{aligned}C_{SM} &= 4180\,MF_{Water} + 1711\,MF_{Protoein} \\ &\quad + 1928\,MF_{Fat} + 1547\,MF_{Carbohydrate} \\ &\quad + 908\,MF_{Ash}\end{aligned} \tag{19}$$

2.3 Experimental procedure

To study the *Spirulina* drying in the proposed dryer, a prototype of the continuous IRARW dryer coupled with the PVT collector was designed and developed in Biosystems Engineering Department of Shahid Bahonar University of Kerman, Iran. The designed dryer has several operating parameters, including *Spirulina* feeding rate, air flow rate, air temperature, water temperature, and IR intensity, which were expected to affect the drying performance and the final quality of the products. According to the literature, temperature and thickness are more important in microalgae drying operations. Dehydrated algae with commercial humidity cannot be obtained at temperatures below 50 °C [23]. On the other hand, *Spirulina* contains phycocyanin compounds and unsaturated fatty acids that the use of high temperatures can reduce their quantity and quality. Phycocyanin

was more highly preserved and the oxidation of unsaturated fatty acids was minimal at < 60 °C of convective hot air, but under extreme temperature conditions, lipid oxidation occurred [24]. The drying rate is highly affected by the sample thickness and the drying temperature, but due to the challenges associated with some labile compounds of *Spirulina*, a temperature of 50 °C was chosen. Since investigating all the other parameters in one study was not possible, a set of pre-tests were organized to find the most effective parameter and its allowable variation ranges, based on the final moisture content, energy consumption, solar heat and electricity fractions, and quality characteristics of the final products. Finally, experimental investigation of the dryer was carried out with two variables: drying air flow rate (0.036, 0.071, and 0.107 $m^3/s/m^2$ collector) and *Spirulina* feeding rate (1.2 L/h, 1.8 L/h, and 2.4 L/h). The variation range of the experiment factors (Spirulina feeding rate and drying air velocity) was selected based on the results of the pre-tests so that the final moisture content of the product would be in the acceptable range of 9–16% wb. The moisture content of lower than 9% wb means that the product gets over-dried. If the moisture content of the product, after discharging from the dryer is higher than 16% wb, it should be kept in room condition for a long time to reach the equilibrium moisture content. During the tests, water pump flow rate, and belt speed were kept constant at 0.5 L/min, and 0.05 m/min, respectively. Based on the results of the pre-tests, only two 200-W IR lamps were engaged during the experiments, covering a length of 65 cm of the drying path. A peristaltic pump was used to spray *Spirulina* at the three different feeding rates on the Mylar surface. Experiments were carried out starting at December 30, 2019, and lasted 37 days. Before each test, the setup was run for two hours at the test condition. Performance evaluation of the proposed design includes evaluation of the PVT collector and the dryer. The PVT collector performance was investigated based on the electrical and thermal efficiencies of the collector. Additionally, the dryer performance was studied using solar electricity and heat fractions, specific energy consumption, specific moisture extraction rate, final moisture content, color indices, and phycocyanin content of the final product. At the end of each experiment, the dried samples were maintained in refrigerated conditions.

2.4 Drying the materials and sample preparation

The stock of *Spirulina maxima*, with an initial optical density (OD) of 0.241 at 680 nm, was prepared and grown in Zarrouk culture medium under controlled conditions [25]. The optical density of samples was measured by spectrophotometer at 680 nm wavelength. The *Spirulina maxima*, with the $OD_{680} = 0.8–0.9$, was harvested and then dewatered using centrifugation at 10,000 rpm for 1 min (Sigma 3-30 K, Osterode am Harz, Germany). The dewatered *Spirulina maxima* samples with the moisture content of 92% wb were stored in a freezer at -18 ± 1 °C. Before each test, the sample of *Spirulina* was located in the room condition (temperature of 25.2 ± 2 °C and relative humidity of 10 ± 0.8%) for two hours. After that, the materials (with an initial moisture content of 90 ± 1.2% wb) were transferred to the feeding system to be dried in the dryer. The products, after discharging from the dryer, were kept in stainless steel containers in room condition for 3–5 h to reach a uniform equilibrium moisture content of 10 ± 1.2% wb.

2.5 Evaluated parameters

The dryer performance was investigated using the thermal and electrical efficiencies of the PVT air collector, solar electricity and heat fraction, specific energy consumption, specific moisture extraction rate, final moisture content, color indices, and phycocyanin content of the final product. The methods for calculating these parameters are given in Table 2.

Table 2 Evaluated parameters and their calculation method

	Parameter	Description	Expression	Reference
1	ζ_{th}	Thermal efficiency of the collector (%)	$\zeta_{th} = \frac{\dot{Q}}{GA_{PV}}$	[26]
2	$\dot{Q}$	The thermal power of the collector (W)	$\dot{Q} = \dot{m}_a C_a (T_o - T_i)$	[27]
3	ζ_{el}	Electrical efficiency of the PVT collector (%)	$\zeta_{el} = \frac{P_{PV}}{GA_{PV}}$	[28]
4	SEC	Specific energy consumption (kWh/kg)	$SEC = \frac{E_T}{m_{wd}}$	[29]
5	SEF	Solar electricity fraction	$SEF = \frac{E_{PV}}{E_T}$	[30]
6	SHF	Solar heat fraction	$SHF = \frac{E_{Sh}}{E_T}$	[31]
7	SMER	Specific moisture extraction rate (kg/kWh)	$SMER = \frac{m_{wd}}{E_T}$	[29]
8	E_{Sh}	The amount of heat energy produced in the photovoltaic-thermal system during the test (Wh)	$E_{Sh} = \int_0^t \dot{Q} dt$	[32]

Table 3 Technical specification and results of uncertainty analysis of the instruments

Instrument (model)	measurement parameter	Accuracy	Uncertainty
Wattmeter (TM1510)	Electrical power consumption	± 1 W	0.58 W
Switched temperature controller (STC-100)	Water temperature	± 1 °C	0.58 °C
Hot-wire anemometer (TES-1341)	Air flow rate	± 3%	1.73%
Pyranometer (TES1333)	Solar irradiance	± 1 W/m^2	0.58 W/m^2
Anemometer (TES1340)	Air velocity (m/s)	± 0.3 m/s	1.73 m/s
PV output (Prova 200A)	PV analyzer		
RH sensor (SUN25-H)	RH of air (%)	± 3%	1.73

To determine the moisture content of the *Spirulina maxima*, the samples were placed in the oven for 18 h at 60 °C, in accordance with the proposed method by Wychen [33].

The color indices of the product, including a* for redness (green to red), L* for lightness (white to black or light to dark), and b* for yellowness (yellow to blue), were measured in each experiment using a colorimeter (TES 135A, TES Co., Taiwan).

The phycocyanin contents of *Spirulina maxima* samples were measured using the method explained by Silva et al. [34]. Distilled water was used as the solvent in the extraction of phycocyanin, and the light absorbance of samples was recorded at 620 nm and 652 nm. The results were presented in units of grams of phycocyanin per 100 g of the dried sample.

2.6 Measurement instrument and uncertainty analysis

Solar radiation on the surface of the collector, ambient temperature, inlet and outlet air temperature, the water temperature, relative humidity of the inlet and outlet air of the dryer, air flow rate inside the dryer's duct, power consumption of the water heater, blower, pump, electrical power generated by the PV panel were measured during the experiments. The standard uncertainty (UC) of the measured parameters was calculated using the following expression [35]:

$$\mathrm{UC} = \frac{\text{Accuracy}}{\sqrt{3}} \tag{20}$$

Table 3 expresses technical specifications of the measurement instruments. Location of the instruments on the dryer is indicated in Fig. 2.

3 Results and discussion

3.1 Irradiance and ambient temperature

Changes in the average ambient temperature and solar irradiance in Kerman city during the experiments are indicated in Fig. 3. As can be seen, the solar irradiance changed from 887.2 to 1167.6 W/m^2 during the course of the study. The minimum and maximum ambient temperatures were 26.12 °C and 29.81 °C, respectively.

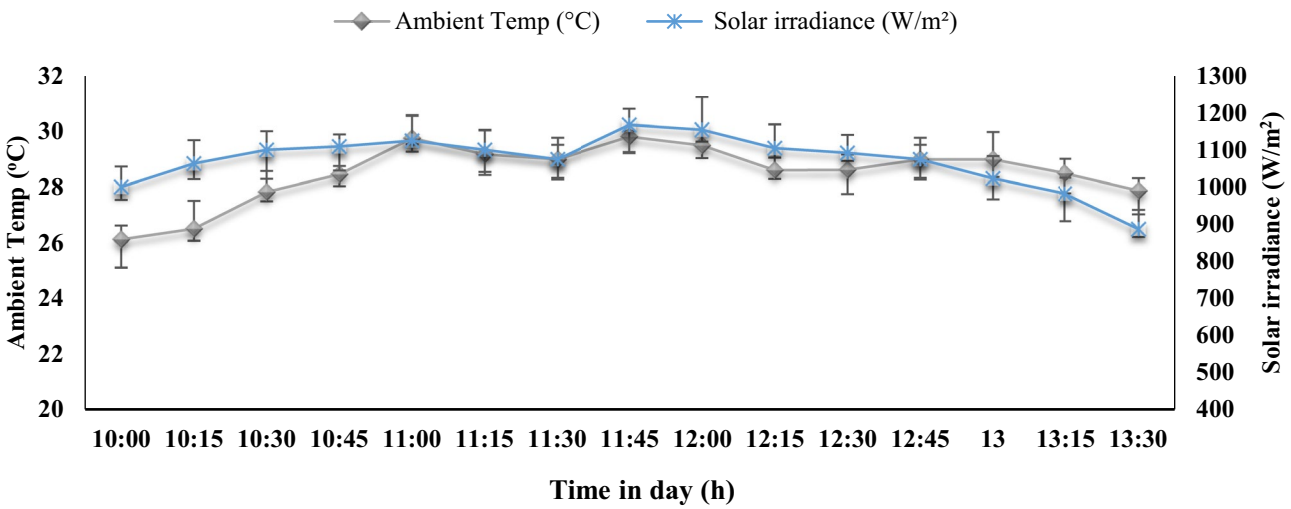


Fig. 3 Changes of the average ambient temperature and solar irradiance in the experiment days in Kerman, Iran

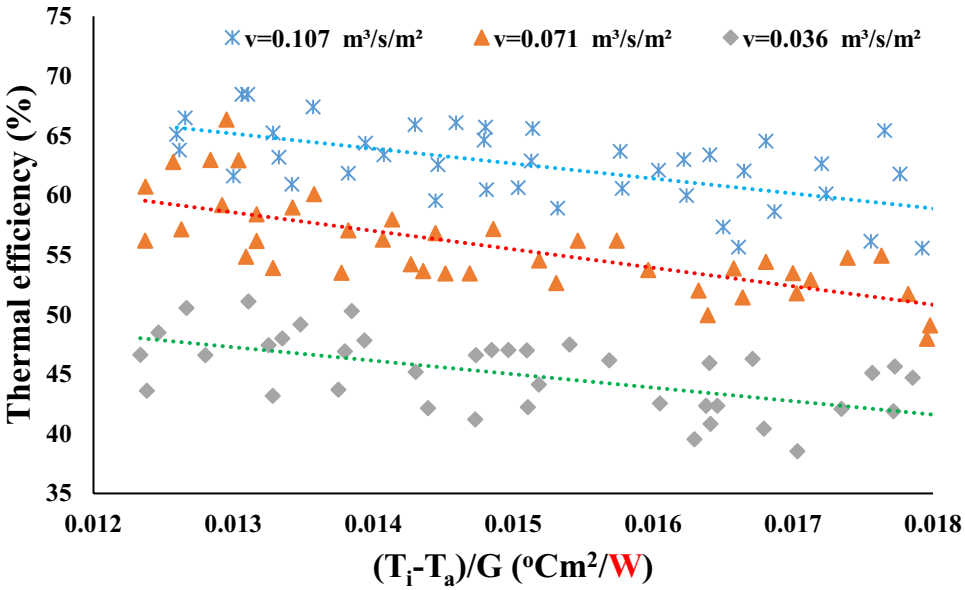


Fig. 4 Thermal efficiency of the PVT collector under the different conditions

3.2 Performance of the PVT collector

Changes in thermal efficiency of the collector based on the change in the difference between the inlet temperature of the panel (T_i) and the ambient temperature (T_a) per unit intensity of solar irradiation (G) are shown in Fig. 4. According to Fig. 4, thermal efficiency increased with raising the air flow rate. As the velocity of the air passing through the collector channel increases, its convective heat transfer coefficient and consequently its ability to absorb and transfer heat from the solar collector increases. This enhances the thermal efficiency of the collector. These findings are in accordance with the results of Dubey et al. [36], and Lee et al. [37]. The maximum thermal efficiency was 68.47% at the air flow rate of 0.107 $m^3/s/m^2$ collector.

Figure 5 shows the effect of the temperature difference per unit solar radiation and air flow rate on electrical efficiency. Increasing the air flow rate from 0.036 to 0.107 $m^3/s/m^2$ collector, increased the electrical efficiency by 13%, mainly due to the reduction of the operating temperature of the PV module. These findings are in accordance with findings reported by Minaei et al. [38]. Table 4 compares the performance of the presented PVT collector with those investigated in the previous studies.

The greatest thermal efficiency (80–95%) was reported by Yandri [41] in the literature, where a hybrid PVT collector was used; however, in his study, no improvement was achieved in terms of electrical efficiency. A double path, dual fluid PVT humidifier also proved to produce a high thermal efficiency at about 76% [40]. Other studies [28,

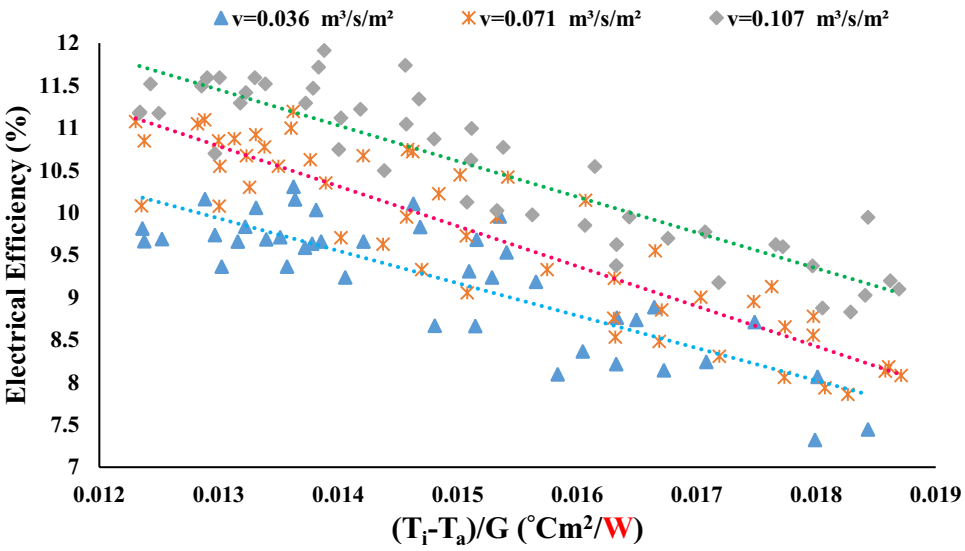


Fig. 5 Electrical efficiency of the PVT collector under the different conditions

Table 4 Comparison of the designed PVT collector with those of literature

Type of PVT collector	Electrical efficiency	Thermal efficiency	Key findings	Reference
Natural flow air collector with phase changed materials (PCM) beneath the PV panel	14.12% and 19.75%	-	25% and 35% reductions in PV cell temperature for PV/PCM and air PVT/PCM systems, respectively, where electrical efficiency of PV cells was 14.12% and 19.75%	[39]
Double path, dual fluid PVT humidifier for the humidification-dehumidification system coupled with heat pump	11.3%	75.6%	Increasing the water flow increased electrical and thermal efficiencies due to the increased evaporation rate	[40]
Hybrid PVT collector with an absorber made from polymethyl methacrylate (PMMA) combined with copper sheet	0.03% /°C decrease	80–95%	PMMA can be used as a good absorber in hybrid PVT collectors and is suitable for low-temperature applications	[41]
greenhouse dryers coupled with PVT air collector	11.26%	56.30%	With increasing air flow rate, the outlet air temperature from PVT decreased, and consequently, the electrical efficiency increased	[42]
PVT water collector design with spiral, web, and direct flow absorber	13.81% for spiral absorber	53.64% for direct absorber	Increasing the mass flow rate decreased the PV temperature which increased both electrical and thermal efficiency	[43]
Glazed photovoltaic thermal tile air collector	12.4%	35.7%	Increasing the radiation intensity increased the temperature of the cell, resulting in a decrease in electrical efficiency	[44]
Parabolic trough photovoltaic/thermal collector with a geometric concentration ratio of 37 ×	11%	58%	Increasing the temperature reduced the efficiency of the system	[28]
Double-pass PVT air collector	11.91%	68.47%	Increasing the air flow rate improved electrical and thermal efficiencies	Present study

42–44] found lower thermal efficiencies than the proposed method of this study, while electrical efficiencies were in the same order, in most of the studies ranging approximately from 11 to 14%. Based on these comparisons, the proposed method was found to be successful to achieve fairly high thermal efficiency (68%), whereas the electrical efficiency was similar to the findings of other methods summarized in Table 4.

3.3 Dryer performance evaluation

3.3.1 Final moisture content

Moisture content of the dried product was measured at the end of each experiment (Fig. 6). The results show that raising the air flow rate to 0.107 $m^3/s/m^2$ collector decreases the final moisture content by 24.5% because of the increase in the moisture evaporation rate as a result of the enhancement of the convective heat transfer coefficient of the moving air. Many studies have shown that evaporation rate increases with increasing air velocity [45, 46]. Moreover, the moisture content of the final product increased by 36.9% with increasing the *Spirulina* feeding rate from 1.2 to 2.4 L/h. Similarly, it was shown in a research that the moisture evaporation rate decreased as the thickness of the product increased [47].

3.3.2 Specific energy consumption and Specific moisture extraction rate

The values of SEC and SMER at the different air flow rates and *Spirulina* feeding rates are shown in Figs. 7 and 8, respectively. Increasing the air flow rate from 0.036 to 0.107 $m^3/s/m^2$ collector decreased the SEC values by 26%. The reason is the growth in the water evaporation rate from the product induced by the enhancement of the air velocity. Raising the feeding rate of the product from 1.2 to 2.4 L/h has increased the SEC by 50.9%. The reason should be the reduction of the evaporation rate because of the increase in the moisture diffusion resistance inside the product with increasing the thickness. On average, the lowest SEC value (1.21 kWh/kg) was observed at the feeding rate of 1.2 L/h and the air flow rate of 0.107 $m^3/s/m^2$ collector. Unlike SEC, the amount of SMER decreased with increasing the feeding rate. Raising the air flow rate increased the SMER. The values of SMER were obtained between 0.41–0.83 kg/kWh. The evaluation results of some solar systems and dryers were given in Table 5.

3.3.3 Solar electricity and heat fraction

Figure 9 illustrates the effect of different air flow rates and *Spirulina* feeding rates on SEF. Raising the air flow rate improved the SEF by reducing total energy consumption

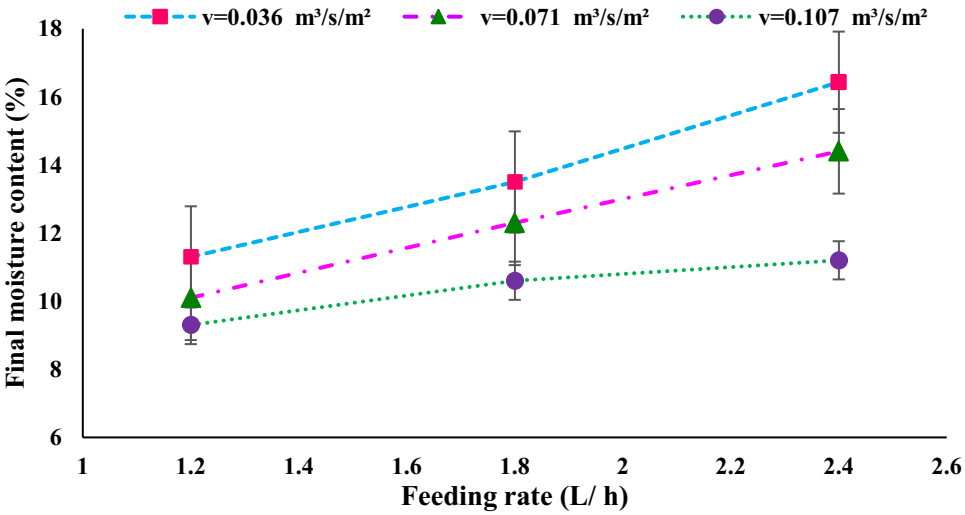


Fig. 6 Moisture content of dried *Spirulina maxima* at the end of each experiment

and increasing the electricity generated by the PVT collector. Since the temperature of the PV module was well reduced, the performance of the PVT was significantly improved. The highest SEF value was 0.761 at the air flow rate of 0.107 $m^3/s/m^2$ collector.

According to Fig. 10, the SHF values decreased by 9.5% when the feeding rate increased from 1.2 to 2.4 L/h. This is related to the increase in the energy consumption with increasing the feeding rate. Similarly, it was found in a research that the amount of SHF decreased as the potatoes' thickness increased [47]. Clearly, raising the air flow rate increased the SHF by improving thermal efficiency of the solar collector, and moisture evaporation rate from the product. The SHF values changed between 0.63 and 0.78. The maximum average SHF was at the air flow rate of 0.107 $m^3/s/m^2$ collector and feeding rate of 1.2 L/h. These findings were compared with those of some other researchers in Table 5.

3.3.4 Color analysis of dried products

According to Fig. 11, the a^* values increased by 39.4% when the feeding rate increased from 1.2 to 2.4 L/h. Increasing the a* by increasing the feeding rate of *Spirulina* means decreasing the greenness of the final product [54–56]. The b^* values decreased by 63.67% when the feeding rate increased from 1.2 to 2.4 L/h. Raising the air flow rate from 0.036 to 0.107 $m^3/s/m^2$ collector also increased the a^* values of samples by 39.3% and decreased the b^* values by 39.2%. The maximum value of L* (53.25) was obtained at the flow rate of 0.107 $m^3/s/m^2$ collector and the feeding rate of 1.2 L/h. Increasing the air flow rate from 0.036 to 0.071 $m^3/s/m^2$ collector and

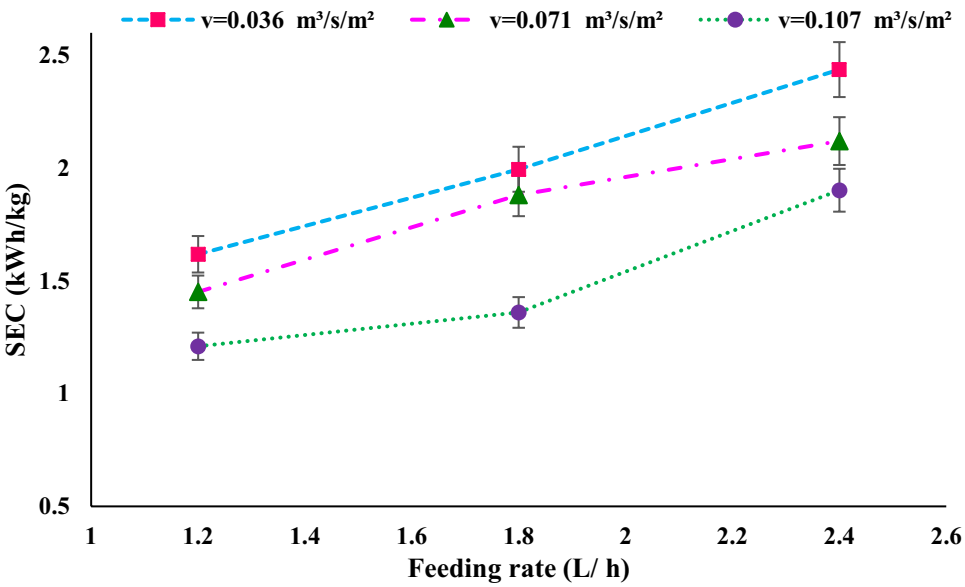


Fig. 7 Specific energy consumption in different drying conditions

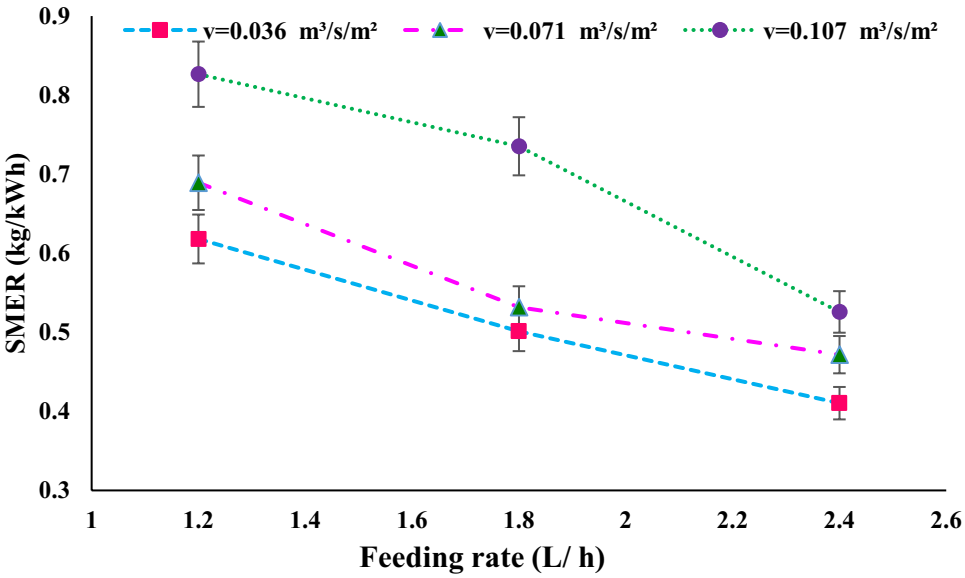


Fig. 8 The specific moisture extraction rate in different drying conditions

0.071 to 0.107 $m^3/s/m^2$ collector increased and decreased the L*, respectively. The L* values at the air flow rate of 0.071 $m^3/s/m^2$ collector increased with the increase in the feeding rate of *Spirulina*. At the other air flow rates, the L* values first descended from the feeding rate of 1.2 to 1.8 L/h and then ascended from 1.8 to 2.4 L/h. In both cases, the final values of L* were lower at the feeding rate of 2.4 L/h compared to 1.2 L/h. Similar fluctuations were observed by other researchers in L* and b* values and color differences [23].

In general, chlorophyll, phycocyanin, and carotenoid pigments represent the green, blue, and yellow-to-red colors of *Spirulina*, respectively [57]. These pigments, along with the physical and superficial properties of dried *Spirulina*, are effective in evaluating the color of samples by affecting the type of light scattering from the surface of the product [58]. Based on the previous findings [23, 33, 59, 60] and the results of the current study, it is concluded that there may not be a definite rule of changes in the color properties of some cases during drying processes due to the natural variabilities of food products and their non-linear behavior because of the complex relations among parameters affecting the process.

The L* reduction with increasing the thickness and aggregation of the mass and collapse of the cell walls along with enzymatic and non-enzymatic browning reactions have been reported in *Spirulina* [58, 61]. At the lower air flow rate (0.036 $m^3/s/m^2$ collector) and consequently higher temperature, the amount of L* was the lowest at all the feeding rates, which can be attributed to the loss of bright color in the samples. The cause can be the formation of brown pigments due to heat and the oxidation of pigment compounds. An alkaline environment, high initial water activity, the presence of iron and copper as well as unsaturated fatty acids in *Spirulina* can help decompose chlorophyll into brown compounds during the drying process [58].

The a* (red-green) of *Spirulina* is affected by carotenoid and chlorophyll pigments and their interaction. The negative value of a* indicates a greener color (higher chlorophyll content), and the positive value indicates a yellow-to-red color

Table 5 The evaluation results of some solar systems and dryers

System description	SEC	SHF	SEF	Reference
Drying of Pistacia Atlantica	6.01–340.97 kWh/kg	-	-	[48]
Solar juice concentration system	3.33–4.07 MJ/kg	0.69–0.74	0.76	[31]
Liquid desiccant-assisted solar dryer for tomato	-	38.5–63.4	0.45–1.7	[30]
Solar dryer equipped with a novel heat recovery system for onion	2.094 kWh/kg	-	-	[49]
PV-solar collector-assisted intermittent IR dryer for tomato	1.79–4.35 kWh/kg	-	-	[47]
Microwave dryer for potato slice	1.172–2.93 kWh/kg	-	-	[50]
PVT solar dryer equipped with Heat pump for saffron	0.86 kWh/kg	0.24–0.67	-	[51]
Drying of the Aloe vera gel	4.31–14.92 kWh/kg	-	-	[52]
Microwave-convective drying	26.32 and 85.45 MJ/kg	-	-	[53]
PVT collector assisted IRARW dryer	1.21–2.437 kWh/kg	0.63 -0.78	0.549–0.761	Present study

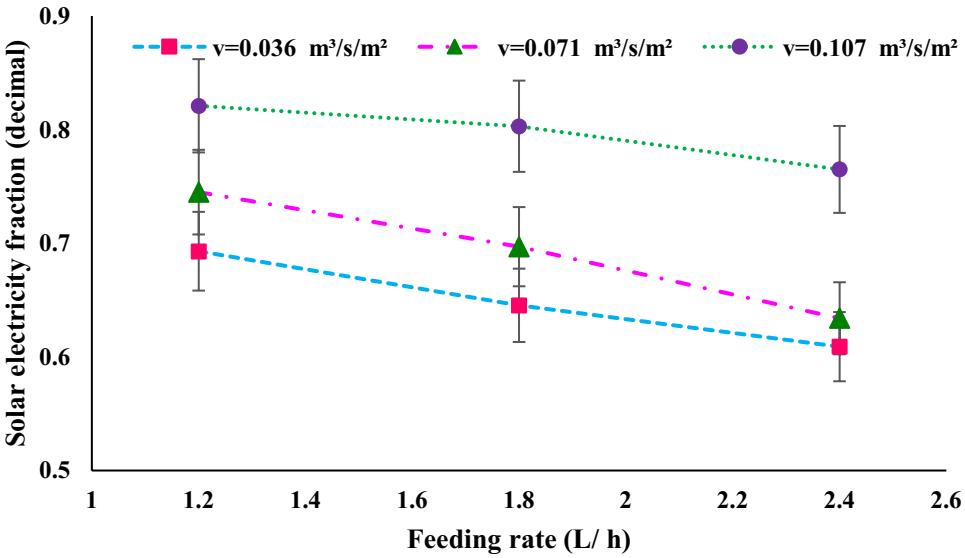


Fig. 9 Changes of SEF with air flow rate and feeding rate of *Spirulina maxima*

of the dried *Spirulina* (more carotenoids). The higher values of a* samples at the higher feeding rates (greater thickness) indicate decomposition of chlorophyll to brown pheophytin or pheophorbide derivatives by active degrading enzymes [58, 61], which is also consistent with the results of L*. Also, the predominance or possible retention of carotenoids compared to the other pigments leads to an increase in the amount of a*. It seems that at the lowest air flow rate (0.036 $m^3/s/m^2$ collector) with the higher temperature and more negative values of the a*, due to the faster inactivation of chlorophyll degrading enzymes and less oxygen contact with the sample, the green color of the dried *Spirulina* is better preserved.

The b* (yellow-blue) is mainly related to carotenoid and phycocyanin pigments. Decreasing the b* with increasing the thickness can be due to the better preservation of pigment compounds, especially phycocyanin. This is because the oxygen contact with the surface and inner parts of the samples is less. A higher value of b* at the air flow rate of 0.036 $m^3/s/m^2$ collector reveals the degradation of phycocyanins and the emergence or retention of carotenoids. The natural carotenoids in *Spirulina* have unsaturated double bonds and all-trans isomers with yellow-to- red color, but their isomerization to cis and oxidation of double bonds significantly reduces their stability and color intensity [62]. It seems that the low air flow rate and less oxygen contact have reduced the oxidation rate of pigment compounds, especially carotenoids. More and in-depth studies may be needed to reveal the driving forces behind the causes and effects of abrupt changes that were observed in Fig. 11.

3.3.5 Phycocyanin content

The drying conditions of *Spirulina* affect its phycocyanin content significantly [63]. As shown in Fig. 12, phycocyanin content kept increasing with the increase in the feeding

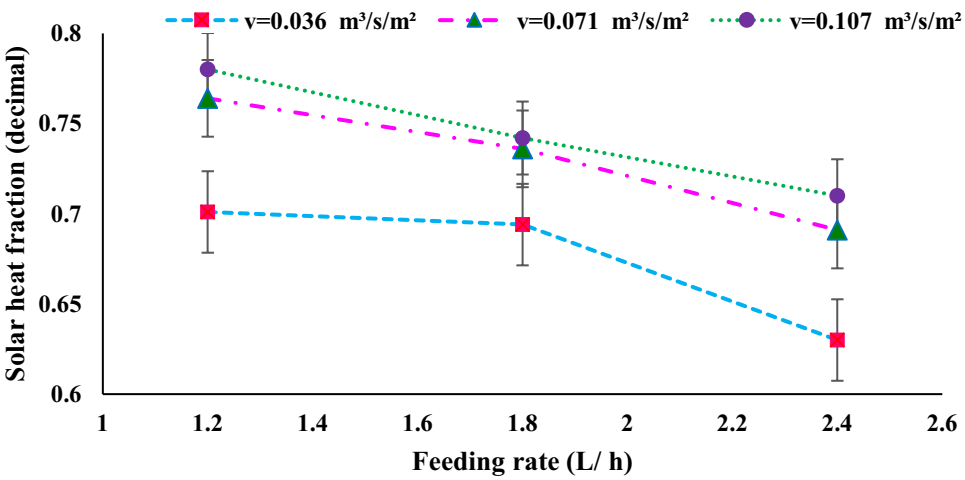


Fig. 10 Changes of SHF with air flow rate and feeding rate of *Spirulina maxima*

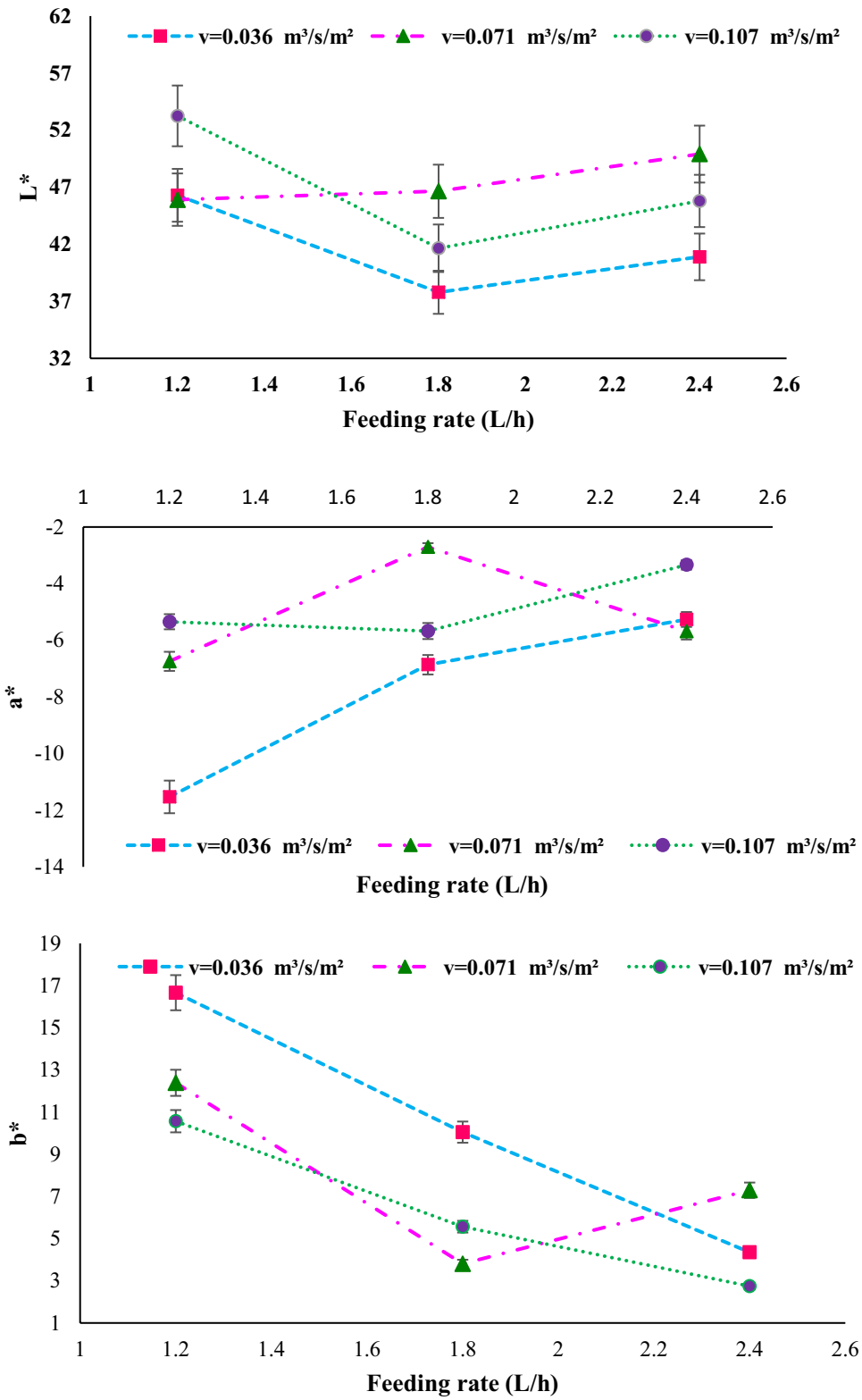


Fig. 11 The color changes of *Spirulina maxima* at different feeding rates and air flow rates, as given by lightness (L*), redness (a*), yellowness (b*)

rate, however the rate of the rise reduced at the air flow rates of greater than 1.8 L/h. Furthermore, the difference in the measured values reduced as the feeding rate increased. In other words, the phycocyanin content increased with rising *Spirulina* feeding rate and air flow rate, probably due to the decrease in the product temperature. The highest amount of phycocyanin (11.46 g/100 g) was observed at the feeding rate of 2.4 L/h and the air flow rate of 0.107 $m^3/s/m^2$ collector.

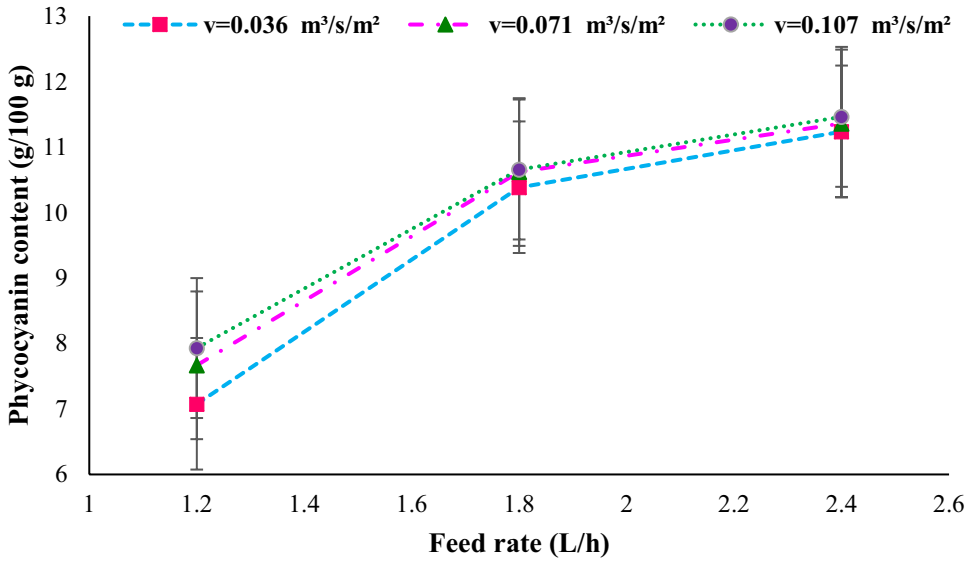


Fig. 12 Variation of phycocyanin content with air flow rate and feeding rate of *Spirulina maxima*

With increasing the feeding rate, in other words, increasing the thickness of the product, in case the product surface is dried, infrared radiation does not reach the middle layers. As a result, the phycocyanin content will be maintained at low temperatures. Furthermore, the content of blue pigment, phycocyanin, is higher in dried samples at the higher air flow rates (0.107 $m^3/s/m^2$ collector), confirmed by the reduced values of the b*. Increasing the air flow rate leads to a decrease in drying temperature, which plays an important role in the preservation or degradation of phycocyanin pigments [23]. The specific chemical structure of phycocyanin makes it thermolabile. This compound is unstable at high temperatures and denatures during drying [61]. The effect of temperature on the degradation of phycocyanin during drying by various methods has been reported by Stramarkou et al. [61].

4 Conclusion

In this study, an infrared-refractance window™ dryer was coupled with a double-pass PVT air collector. Performance evaluation of the dryer was conducted by drying of *Spirulina maxima* microalgae at three levels of drying air flow rate and three levels of *Spirulina* feeding rate. The results revealed that:

- The highest thermal and electrical efficiencies of the PVT collector were 68.47% and 11.91%, respectively. Increasing the air flow rate improved both thermal and electrical efficiencies.
- The average SEC values were between 1.21 and 2.437 kWh/kg, and the maximum SMER value was around 0.83 kg/kWh.
- Raising the air flow rate improved the SEF. The highest SEF value (0.761) was observed at the air flow rate of 0.107 $m^3/s/m^2$ collector.
- Raising the feeding rate from 1.2 to 2.4 L/h reduced the SHF values. Also, the SHF increased with raising the air flow rate. The average SHF values ranged between 0.63 and 0.78.
- The b^* values decreased by 63.67% and the a^* values increased by 39.4% when the feeding rate increased from 1.2 to 2.4 L/h.
- The final moisture content was decreased by 24.5% with increasing the air flow rate from 0.036 to 0.107 $m^3/s/m^2$ collector.
- The highest phycocyanin content was found to be 11.46 g/100 g at the feeding rate of 2.4 L/h and the air flow rate of 0.107 $m^3/s/m^2$ collector.
- Based on the suitable amounts of final moisture content, SEC, and solar fractions as well as the fair quality of the dried products, the air flow rate of 0.107 $m^3/s/m^2$ collector and the feeding rate of 1.2 L/h are recommended for *Spirulina* drying in the designed dryer.

Acknowledgements The authors would like to acknowledge the Research Council of Shahid Bahonar University of Kerman for financial support.

Authors' contributions Zeinab Rezvani—Design and development of the concept, carrying out the experiments, writing the manuscript. Hamid Mortezapour—Supervising the project, discussing the results and contribution to the final manuscript. Mehran Ameri—Helping supervise the project, discussing the results, and contributing to the final manuscript. Hamid-Reza Akhavan—Helping supervise the project, discussing the food analysis results, and contributing to the final manuscript. Selçuk Arslan—Contributing to the final manuscript.

Funding The authors did not receive any fund for this study.

Availability of data and material The datasets used and/or analyzed during the current study are available from the corresponding author on reasonable request.

Code availability Not applicable.

Declarations

Ethics approval Not applicable.

Consent to participate Not applicable.

Consent for publication Not applicable.

Conflict of interest statement I declare no conflict of interest, and my agreement for submission of this manuscript and I claim that this work is novel and has not been submitted elsewhere.

References

1. Costa JAV, Freitas BCB, Rosa GM, Moraes L, Morais MG, Mitchell BG (2019) Operational and economic aspects of *Spirulina*-based biorefinery. Bioresour Technol 292:121946. https://doi.org/10.1016/j.biortech.2019.121946
2. Rodriguez-Concepcion M, Avalos J, Bonet ML, Boronat A, Gomez-Gomez L, Hornero-Mendez D, Limon MC, Meléndez-Martínez AJ, Olmedilla-Alonso B, Palou A (2018) A global perspective on carotenoids: Metabolism, biotechnology, and benefits for nutrition and health. Prog Lipid Res 70:62–93. https://doi.org/10.1016/j.plipres.2018.04.004
3. Sathasivam R, Radhakrishnan R, Hashem A, Abd_Allah EF (2019) Microalgae metabolites: A rich source for food and medicine. Saudi J Biol Sci 26:709 722. https://doi.org/10.1016/j.sjbs.2017.11.003
4. Koyande AK, Chew KW, Rambabu K, Tao Y, Chu D-T, Show P-L (2019) Microalgae: A potential alternative to health supplementation for humans. Food Sci Hum Wellness 8:16–24. https://doi.org/10.1016/j.fshw.2019.03.001
5. Lafarga T, Fernández-Sevilla JM, González-López C, Acién-Fernández FG (2020) *Spirulina* for the food and functional food industries. Food Res Int 137:109356. https://doi.org/10.1016/j.foodres.2020.109356
6. Pragati S, Preeti B (2014) Technological revolution in drying of fruit and vegetables. Int J Sci Res 3:705–711
7. Bernaert N, Van Droogenbroeck B, Van Pamel E, De Ruyck H (2019) Innovative refractance window drying technology to keep nutrient value during processing. Trends Food Sci Technol 84:22–24. https://doi.org/10.1016/j.tifs.2018.07.029
8. Koşan M, Demirtaş M, Aktaş M, Dişli E (2020) Performance analyses of sustainable PV/T assisted heat pump drying system. Sol Energy 199:657–672. https://doi.org/10.1016/j.solener.2020.02.040
9. Mirzaei S, Ameri M, Ziaforoughi A (2021) Energy-exergy analysis of an infrared dryer equipped with a photovoltaic-thermal collector in glazed and unglazed modes. Renew Energy 169:541–556. https://doi.org/10.1016/j.renene.2021.01.046
10. Krishnamoorthi S, Prabhahar M, Madhavan V, Pragathish T, Johnson F (2020) Effect of variation in injector nozzle holes on the performance of preheated *Spirulina* methyl ester used in VCR engine. Mater Today: Proc 45:5840–5846. https://doi.org/10.1016/j.matpr.2020.08.270
11. Franco S, Jaques A, Pinto M, Fardella M, Valencia P, Núñez H, Ramírez C, Simpson R (2019) Dehydration of salmon (*Atlantic salmon*), beef, and apple (*Granny Smith*) using Refractance window™: Effect on diffusion behavior, texture, and color changes. Innov Food Sci Emerg Technol 52:8–16. https://doi.org/10.1016/j.ifset.2018.12.001
12. Jimena Ortiz-Jerez M, Gulati T, Datta AK, Isabel Ochoa-Martinez C (2015) Quantitative understanding of Refractance Window (TM) drying. Food Bioprod Process 95:237–253. https://doi.org/10.1016/j.fbp.2015.05.010
13. Rezvani Z, Mortezapour H, Ameri M, Akhavan H-R, Arslan S (2022) Optimization of tomato slices drying in a continuous infrared-assisted Refractance Window ™ dryer using response surface methodology. Iran J Chem Chem Eng. https://doi.org/10.30492/IJCCE.2022.538139.4914
14. Seyyed Abadi MM, Asadi Amirabadi A, Taheri A, Kashaninezhad M (2016) Investigation of infrared radiation on drying kinetics and color indexes of Anaryjeh (*Froriepia subpinnata*) leaf. Innov Food Technol 4:45–57. https://dx.doi.org/10.22104/jift.2016.339
15. Hegazy MM, El-Sebaii A, Ramadan MR, Aboul-Enein S, Khallaf AE-M (2020) Comparative study of three different designs of a hybrid PV/T double-pass finned plate solar air heater. Environ Sci Pollut Res 27:32270–32282. https://doi.org/10.1007/s11356-019-07487-8
16. Othman M, Yatim B, Sopian K, Bakar M (2006) Double-pass photovoltaic-thermal solar collector. J Energy Eng 132:121–126. https://doi.org/10.1016/j.renene.2004.10.007
17. Hegazy AA (2000) Comparative study of the performances of four photovoltaic/thermal solar air collectors. Energy Convers Manage 41:861–881. https://doi.org/10.1016/S0196-8904(99)00136-3
18. Duffie JA, Beckman WA, Blair N (2020) Solar engineering of thermal processes, photovoltaics and wind. John Wiley & Sons, New Jersey
19. Mortezapour H, Ghobadian B, Minaei S, Khoshtaghaza MH (2012) Saffron drying with a heat pump–assisted hybrid photovoltaic–thermal solar dryer. Drying Technol 30:560–566. https://doi.org/10.1080/07373937.2011.645261
20. Yeh HM, Ho CD, Hou JZ (2002) Collector efficiency of double-flow solar air heaters with fins attached. Energy 27:715–727. https://doi.org/10.1016/S0360-5442(02)00010-5
21. Bergman TL, Lavine AS, Incropera FP, DeWitt DP (2011) Introduction to heat transfer. John Wiley & Sons, USA
22. Heldman DR, Gorby D (1975) Prediction of thermal conductivity in frozen foods. Trans ASAE 18:740–0744. https://doi.org/10.13031/2013.36674
23. Costa BR, Rodrigues MC, Rocha SF, Pohndorf RS, Larrosa AP, Pinto LA (2016) Optimization of *Spirulina* sp. drying in heat pump: effects on the physicochemical properties and color parameters. J Food Process Preserv 40:934–942. https://doi.org/10.1111/jfpp.12672
24. Oliveira EG, Duarte JH, Moraes K, Crexi VT, Pinto LA (2010) Optimisation of *Spirulina platensis* convective drying: evaluation of phycocyanin loss and lipid oxidation. Int J Food Sci Tech 45:1572–1578. https://doi.org/10.1111/j.1365-2621.2010.02299.x
25. Zarrouk C (1966) Contribution aletude dune cyanophycée influence de divers facteurs physiques et chimiques surla croissance etla photosynthèse de *Spirulina maxima* (Setch. et Gardner) Geitler (Ph. D. thèsis). University of Paris
26. Duffie JA, Beckman WA (1980) Solar engineering of thermal processes. John Wiley & Sons, New Jersey
27. Eltawil MA, Azam MM, Alghannam AO (2018) Solar PV powered mixed-mode tunnel dryer for drying potato chips. Renew

Energy 116:594–605. https://doi.org/10.1016/j.renene.2017.10.007
28. Coventry JS (2005) Performance of a concentrating photovoltaic/thermal solar collector. Sol Energy 78:211–222. https://doi.org/10.1016/j.solener.2004.03.014
29. Coşkun S, Doymaz I, Tunçkal C, Erdoğan S (2017) Investigation of drying kinetics of tomato slices dried by using a closed loop heat pump dryer. Heat Mass Transfer 53:1863–1871. https://doi.org/10.1007/s00231-016-1946-7
30. Dorouzi M, Mortezapour H, Akhavan H-R, Moghaddam AG (2018) Tomato slices drying in a liquid desiccant-assisted solar dryer coupled with a photovoltaic-thermal regeneration system. Sol Energy 162:364–371. https://doi.org/10.1016/j.solener.2018.01.025
31. Alizadeh H-R, Mortezapour H, Akhavan H-R, Balvardi M (2019) Performance of a liquid desiccant-assisted solar juice concentration system for barberry juice. Sol Energy 184:1–10. https://doi.org/10.1016/j.solener.2019.03.085
32. Eltawil MA, Azam MM, Alghannam AO (2018) Energy analysis of hybrid solar tunnel dryer with PV system and solar collector for drying mint (*Mentha Viridis*). J Clean Prod 181:352–364. https://doi.org/10.1016/j.jclepro.2018.01.229
33. Hosseinizand H, Sokhansanj S, Lim CJ (2018) Studying the drying mechanism of microalgae *Chlorella vulgaris* and the optimum drying temperature to preserve quality characteristics. Drying Technol 36:1049–1060. https://doi.org/10.1080/07373937.2017.1369986
34. Silva NC, Duarte CR, Barrozo MA (2020) Analysis of the use of a non-conventional rotary drum for dehydration of microalga *Spirulina platensis*. Bioprocess Biosystems Eng 43:1–9. https://doi.org/10.1007/s00449-020-02329-1
35. Siddiqui FR, Elminshawy NA, Addas MF (2016) Design and performance improvement of a solar desalination system by using solar air heater: Experimental and theoretical approach. Desalination 399:78–87. https://doi.org/10.1016/j.desal.2016.08.015
36. Dubey S, Solanki S, Tiwari A (2009) Energy and exergy analysis of PV/T air collectors connected in series. Energy Build 41:863–870. https://doi.org/10.1016/j.enbuild.2009.03.010
37. Lee JH, Hwang SG, Lee GH (2019) Efficiency improvement of a photovoltaic thermal (PVT) system using nanofluids. Energies 12:1–16. https://doi.org/10.3390/en12163063
38. Minaei S, Motevali A, Ghobadian B, Banakar A, Samadi SH (2014) An investigation of energy consumption, solar fraction and hybrid photovoltaic–thermal solar dryer parameters in drying of chamomile flower. Int J Food Eng 10:697–711. https://doi.org/10.1515/ijfe-2014-0135
39. Singh AP, Kumar A, Singh OP (2020) Effect of natural convection and thermal storage system on the electrical and thermal performance of a hybrid PV-T/PCM systems. Mater Today: Proc 39:1899–1904. https://doi.org/10.1016/j.matpr.2020.08.010
40. Pourafshar ST, Jafarinaemi K, Mortezapour H (2020) Development of a photovoltaic-thermal solar humidifier for the humidification-dehumidification desalination system coupled with heat pump. Sol Energy 205:51–61. https://doi.org/10.1016/j.solener.2020.05.045
41. Yandri E (2019) Development and experiment on the performance of polymeric hybrid Photovoltaic Thermal (PVT) collector with halogen solar simulator. Sol Energy Mater Sol Cells 201:110066. https://doi.org/10.1016/j.solmat.2019.110066
42. Tiwari S, Agrawal S, Tiwari GN (2018) PVT air collector integrated greenhouse dryers. Renew Sust Energ Rev 90:142–159. https://doi.org/10.1016/j.rser.2018.03.043
43. Fudholi A, Sopian K, Yazdi MH, Ruslan MH, Ibrahim A, Kazem HA (2014) Performance analysis of photovoltaic thermal (PVT) water collectors. Energy Convers Manage 78:641–651. https://doi.org/10.1016/j.enconman.2013.11.017
44. Agrawal S, Tiwari G, Pandey H (2012) Indoor experimental analysis of glazed hybrid photovoltaic thermal tiles air collector connected in series. Energy Build 53:145–151. https://doi.org/10.1016/j.enbuild.2012.06.009
45. Putra RN, Ajiwiguna TA (2017) Influence of air temperature and velocity for drying process. Procedia Eng 170:516–519. https://doi.org/10.1016/j.proeng.2017.03.082
46. Uddin Z, Suppakul P, Boonsupthip W (2016) Effect of air temperature and velocity on moisture diffusivity in relation to physical and sensory quality of dried pumpkin seeds. Drying Technol 34:1423–1433. https://doi.org/10.1080/07373937.2015.1119840
47. Ziaforoughi A, Esfahani JA (2016) A salient reduction of energy consumption and drying time in a novel PV-solar collector-assisted intermittent infrared dryer. Sol Energy 136:428–436. https://doi.org/10.1016/j.solener.2016.07.025
48. Kaveh M, Chayjan RA, Taghinezhad E, Sharabiani VR, Motevali A (2020) Evaluation of specific energy consumption and GHG emissions for different drying methods (Case study: *Pistacia Atlantica*). J Clean Prod 259:120963. https://doi.org/10.1016/j.jclepro.2020.120963
49. Mortezapour H, Rashedi S, Akhavan H, Maghsoudi H (2018) Experimental analysis of a solar dryer equipped with a novel heat recovery system for onion drying. J Agric Sci Technol 19:1227–1240
50. Darvishi H (2012) Energy consumption and mathematical modeling of microwave drying of potato slices. Agric Eng Int: CIGR J 14:94–102
51. Mortezapour H, Ghobadian B, Minaei S, Khoshtaghaza MH (2012) Saffron drying with a heat pump–assisted hybrid photovoltaic–thermal solar dryer. Dry Technol 30:560–566. https://doi.org/10.1080/07373937.2011.645261
52. Motevali A, Minaei S, Khoshtaghaza MH, Amirnejat H (2011) Comparison of energy consumption and specific energy requirements of different methods for drying mushroom slices. Energy 36:6433–6441. https://doi.org/10.1016/j.energy.2011.09.024
53. Sharma G, Prasad S (2006) Specific energy consumption in microwave drying of garlic cloves. Energy 31:1921–1926. https://doi.org/10.1016/j.energy.2005.08.006
54. Pool EK, Shahidi F, Mortazavi SA, Azizpour M, Daneshzad E (2016) Examination of the effect of *Spirulina platensis* microalgae on drying kinetics and the color change of kiwifruit pastille. J Food Meas Charact 10:634–642. https://doi.org/10.1007/s11694-016-9347-7
55. Fradique M, Batista AP, Nunes MC, Gouveia L, Bandarra NM, Raymundo A (2010) Incorporation of *Chlorella vulgaris* and *Spirulina maxima* biomass in pasta products. Part 1: Preparation and evaluation. J Sci Food Agric 90:1656–1664. https://doi.org/10.1002/jsfa.3999
56. Sousa I, Gouveia L, Batista AP, Raymundo A, Bandarra NM (2008) Microalgae in novel food products. Food Chem Res Develop 75–112
57. Park WS, Kim HJ, Li M, Lim DH, Kim J, Kwak SS, Kang CM, Ferruzzi MG, Ahn MJ (2018) Two classes of pigments, carotenoids and c-phycocyanin, in spirulina powder and their antioxidant activities. Molecules 23:2065. https://doi.org/10.3390/molecules23082065
58. Nouri E, Abbasi H, Rahimi E (2018) Effects of processing on stability of water-and fat-soluble vitamins, pigments (C-phycocyanin, carotenoids, chlorophylls) and colour characteristics of *Spirulina platensis*. Qual Assur Saf Crop 10:335–349. https://doi.org/10.3920/QAS2018.1304
59. Khazaei Pool E, Shahidi F, Mortazavi SA, Azizpour M, Daneshzad E (2016) Examination of the effect of *Spirulina platensis* microalgae on drying kinetics and the color change of kiwifruit pastille. J Food Meas Charact 10:634–642. https://doi.org/10.1007/s11694-016-9347-7

60. Tello-Ireland C, Lemus-Mondaca R, Vega-Gálvez A, López J, Di Scala K (2011) Influence of hot-air temperature on drying kinetics, functional properties, colour, phycobiliproteins, antioxidant capacity, texture and agar yield of alga *Gracilaria chilensis*. LWT-Food Sci Technol 44:2112–2118. https://doi.org/10.1016/j.lwt.2011.06.008
61. Stramarkou M, Papadaki S, Kyriakopoulou K, Tzovenis I, Chronis M, Krokida M (2021) Comparative analysis of different drying techniques based on the qualitative characteristics of *Spirulina platensis* biomass. J Aquat Food Prod Technol 30:498–516. https://doi.org/10.1080/10498850.2021.1900969
62. Shi J, Maguer ML (2000) Lycopene in tomatoes: chemical and physical properties affected by food processing. Crit Rev Food Sci Nutr 40:1–42. https://doi.org/10.1080/10408690091189275
63. de Farias NF, Demarco M, Tribuzi G (2019) Drying and quality of microalgal powders for human alimentation. In: Vítová M (ed) Microalgae-from physiology to application. IntechOpen, London, pp 71–88

Publisher's Note Springer Nature remains neutral with regard to jurisdictional claims in published maps and institutional affiliations.